2001 Mars Odyssey Orbit Determination During Interplanetary Cruise

P. G. Antreasian,* D. T. Baird,† J. S. Border,‡ P. D. Burkhart,§ E. J. Graat,¶
M. K. Jah,** R. A. Mase,†† T. P. McElrath,‡‡ and B. M. Portock§§
Jet Propulsion Laboratory, California Institute of Technology, Pasadena, California 91109

On 24 October 2001 coordinated universal time, following a seven-month journey to Mars, Odyssey executed a nominal orbit insertion burn to be captured successfully into orbit around Mars. The excellent navigation performance during the interplanetary cruise resulted in arrival conditions over the north pole of Mars well within $1-\sigma$ of the designed values. The achieved altitude above the north pole was less than 1 km away from the 300-km target altitude. Several sources of error made the orbit determination process for Odyssey challenging. The largest of these errors was caused by the periodic autonomous angular momentum desaturation events. Several navigational aids were brought forth to mitigate the error sources and improve the accuracy of Odyssey's interplanetary cruise navigation. The most significant of these included the incorporation of very long baseline interferometry, delta-differential one-way range tracking data into the orbit determination filtering process and the placement of the spacecraft into a low-torque attitude during the final two months of interplanetary cruise. Orbit determination solution consistency was routinely evaluated through a battery of filter strategies and data combinations. The orbit determination processes and results of Mars Odyssey from launch to orbit insertion at Mars are discussed.

Nomenclature

$B \cdot R$	=	component of B vector (hyperbolic miss vector) along R axis, km
$B \cdot T$	=	component of B vector (hyperbolic miss vector) along T axis, km
α	=	right ascension, deg
ΔDOR	=	delta-differential one-way range, angular measurement made using very long baseline interferometry techniques, ns
ΔV	=	delta velocity, m/s
δ	=	declination, deg

Introduction

NASA's Mars Odyssey spacecraft (S/C) was launched on 7 April 2001 into a type 1 transfer orbit to Mars. Four trajectory correction maneuvers (TCMs) were performed to achieve the required arrival conditions at Mars. On 24 October 2001, 0230 military time,

*Member of Engineering Staff, Mail Stop 230-205, Navigation and Mission Design Section, 4800 Oak Grove Drive.

†Member of Engineering Staff, Mail Stop 264-380, Navigation and Mission Design Section, 4800 Oak Grove Drive. Member AIAA.

‡Principal Engineer, Mail Stop 238-600, Tracking Systems and Applications Section, 4800 Oak Grove Drive.

§Member of Engineering Staff, Mail Stop 301-125L, Navigation and Mission Design Section, 4800 Oak Grove Drive. Senior Member AIAA.

¶Member of Engineering Staff, Mail Stop 264-380, Navigation and Mission Design Section, 4800 Oak Grove Drive.

**Member of Engineering Staff, Mail Stop 264-820, Navigation and Mission Design Section, 4800 Oak Grove Drive. Member AIAA.

††Mission Manager, Mail Stop 264-282, Mars Odyssey Project, 4800 Oak Grove Drive.

‡‡Inner Planet Navigation Group Supervisor, Mail Stop 301-276, Navigation and Mission Design Section, 4800 Oak Grove Drive.

§§Member of Engineering Staff, Mail Stop 301-276, Navigation and Mission Design Section, 4800 Oak Grove Drive. Member AIAA.

after the nearly seven-month journey, Odyssey executed a nominal Mars orbit insertion burn (MOI) to be captured into an 18.6-h orbit. Aerobraking was then employed for nearly three months to reduce the spacecraft's orbital period to 2 h and trim the orbit for science mapping. The Mars Odyssey project is managed at the Jet Propulsion Laboratory (JPL). The spacecraft was built by Lockheed Martin Astronautics (LMA) in Denver, Colorado. The flight team is split between the two institutions because navigation is performed at JPL, whereas the spacecraft subsystem analysts are located at LMA in Denver.

Odyssey Mission

The Odyssey mission objectives are to map globally the chemical elements and mineral distributions that constitute the surface of Mars using the thermal emission imaging system (THEMIS) and gamma ray spectrometer instruments. These instruments will search for evidence of subsurface water ice through the determination of hydrogen and minerals that are known to occur in the presence of water. The Mars radiation environment experiment instrument will study the radiation environment in low Mars orbit to ascertain the radiation risk to future human explorers. Toward the end of its planned 2.5-year science mission, the orbiter will provide an important telecommunications link with Earth for U.S. and international landers and rovers through its uhf relay.

This paper will focus on the details of the orbit determination (OD) that was performed during the cruise phase of the mission. A more general treatment of the Odyssey navigation approach including all mission phases from launch, through orbit insertion, aerobraking and mapping is given by Mase et al.[1] Smith and Bell[2] describe the detailed navigation processes and results during Odyssey's aerobraking phase. Note that all activities referred to in this paper occurred in the year 2001.

MOI Targeting Requirements

After two failed attempts to explore Mars with the Mars Climate Orbiter (MCO) and the Mars Polar Lander. NASA was under tremendous pressure to succeed with Mars Odyssey. The success of Mars Odyssey navigation effort was primarily contingent on accurately determining the spacecraft's orbit during the seven-month cruise and targeting the TCMs to achieve the required Mars encounter conditions necessary for a safe and successful capture into orbit. The mission target requirements were to achieve an encounter periapsis altitude of 405 ± 25 km over the north pole of Mars with

an inclination with respect to the Mars mean equator of date (MME) coordinate frame of 93.467 deg ± 0.2 deg (Refs. 1 and 3). Given that the periapsis altitude would drop by 105 km as a result of the constant pitch-rate MOI burn, the requirement was also given in terms of a P2 periapsis altitude after the first orbit about Mars of 300 km.

Navigational Challenges

Several sources of error made the OD process during cruise challenging for Odyssey. The largest of these errors was caused by the periodic thrusting events brought about by autonomous angular momentum desaturation (AMD) events. AMDs or desaturations were performed every 16–25 h to desaturate the momentum buildup on the reaction wheels caused primarily by solar pressure torque. The thrust vectors of the reaction control system (RCS) attitude thrusters with respect to the S/C's center of mass were not balanced and resulted in a net translational ΔV. These desaturations produced ΔV components orthogonal to the Earth–S/C direction that were not observable with traditional Doppler and range data. It was this source of error (along with the English–metric units conversion) that contributed to the MCO navigation difficulties.

Another source of error affecting Odyssey navigation was caused by the noise and quality of the two-way, X-band Doppler and range tracking data from NASA's Deep Space Network (DSN) antennas. The extreme negative declination of the interplanetary trajectory constrained the tracking of Odyssey to DSN's Canberra, Australia, complex for the first two months of cruise. During this time, several S/C activities were performed to check S/C health and calibrate science instruments and subsystems. These activities routinely corrupted the OD solutions and challenged the OD processes. Eventually, DSN's Goldstone, California, and Madrid, Spain, complexes could track Odyssey through the remainder of cruise but only at low elevations. Tracking data collected at such low elevations were more susceptible to uncalibrated ionospheric and tropospheric conditions, which also may have been exacerbated by higher than usual solar activity at the time. Apart from the occasional noisy tracking pass, the Doppler residual data frequently exhibited an unusual structure that also had the potential of corrupting the OD solutions and producing inconsistent results. These signatures could not be attributed to any S/C activity.

Navigational Aids

Several navigational aids were brought forth to mitigate the aforementioned error sources and improve the accuracy of Odyssey's interplanetary cruise navigation. These include the incorporation of delta-differential one-way range (ΔDOR) tracking data, a type of very long baseline interferometry measurement, into the OD filtering process, active and passive RCS thruster calibrations, solar pressure calibration, differenced range vs integrated Doppler (DRVID) measurements for media calibration, and repositioning the S/C's final cruise attitude into a low-torque orientation. The most significant of these were the ΔDOR measurements and the low-torque configuration. The ΔDOR data type complements the traditional two-way X-band Doppler and range radio-metric measurements by constraining the S/C's position in the Earth plane-of-sky coordinate frame. In addition, the ΔDOR measurements are not dependent on modeling S/C dynamics. Thus, the out-of-the-ecliptic-plane component of Odyssey's position, which is weakly observable with Doppler and range, can be determined from the ΔDOR data. The reduction of the S/C's position uncertainty in this direction was important in meeting the altitude requirement above the north pole of Mars for orbit insertion. The adjustment of the S/C's attitude and solar array to balance solar pressure torque with respect to the center of mass during the last two months of cruise significantly decreased the occurrence of AMDs and effectively removed the desaturation ΔV as being a significant error contributor in the OD solutions for the final targeting maneuver.

Cruise Navigation

Odyssey was launched into a type 1 trajectory toward Mars aboard a Boeing Delta 2 7925 launch vehicle from NASA Kennedy Space
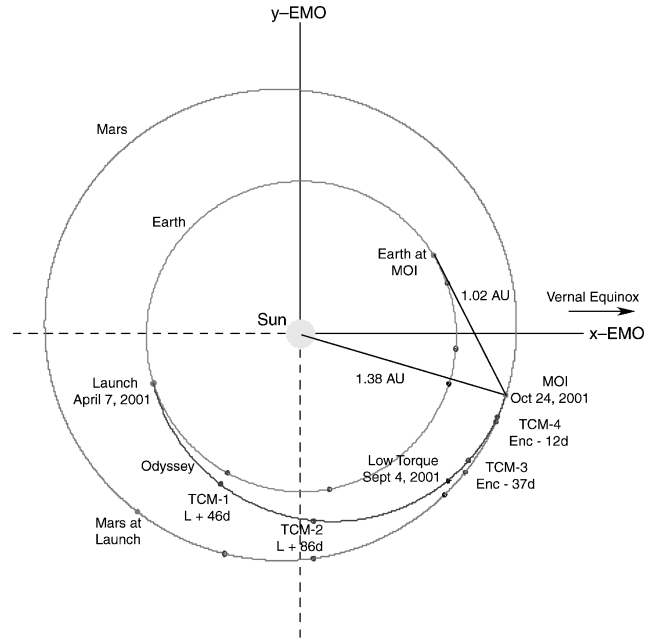
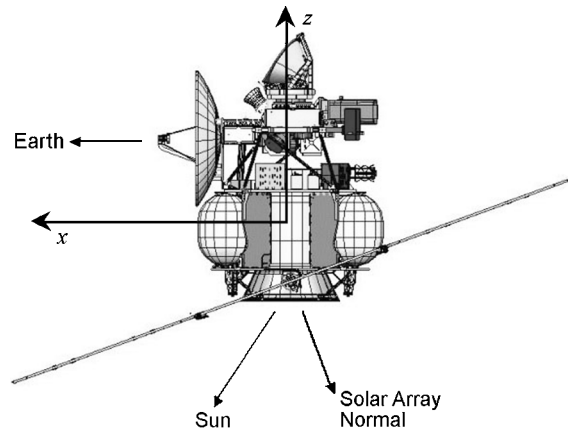

Fig. 1   North ecliptic view of Odyssey's flight path.

Fig. 2   S/C cruise configuration, HGA and *x*-body axis pointed toward Earth, *z* axis pointed away from sun, and solar arrays 55 deg from sun.

Center. The Mars injection target was biased to miss Mars by approximately 450,000 km to ensure that the S/C and the launch vehicle's upper stage would not be on an impacting trajectory, thereby satisfying planetary quarantine requirements (< 10–4 probability of impact). Four TCMs were scheduled during interplanetary cruise to guide Odyssey's flight path to the final B-plane aimpoint and meet the navigational requirements for MOI. The B-plane coordinate frame is an asymptotic coordinate frame centered at the target body with axes S, T, and R used for targeting planetary encounters. In this system, the S vector is aligned parallel to the spacecraft approach asymptote, the T vector is normal to S and parallel to the MME, and R is orthogonal to both S and T, such that $R = S \times T$. The B vector, which lies in the R–T plane, defines the B plane and points from the origin of the coordinate frame to the point where the incoming asymptote intercepts the R–T plane.

Figure 1 shows Odyssey's interplanetary cruise trajectory with respect to Earth and Mars in a north ecliptic view. The Odyssey S/C is shown in Fig. 2. In the case of a contingency, a fifth TCM was planned for, but not executed, in the final day before encounter.

Small Forces

The spacecraft is three-axis stabilized, with three orthogonally mounted reaction wheels (and a spare skew wheel) that spin to absorb excess angular momentum produced primarily by solar

Table 1   RCS thrust vectors in the S/C coordinate frame

Thruster	x	y	z
RCS-1	−0.8926	0.4162	−0.1736
RCS-2	−0.8926	−0.4162	−0.1736
RCS-3	0.8926	−0.4162	−0.1736
RCS-4	0.8926	0.4162	−0.1736

Table 2   RCS thrusters required per wheel desaturation

To produce	Fire	Removes
$-x$ Torque	RCS-2, RCS-3	$+x$ Wheel torque
$+x$ Torque	RCS-1, RCS-4	$-x$ Wheel torque
$-y$ Torque	RCS-3, RCS-4	$+y$ Wheel torque
$+y$ Torque	RCS-1, RCS-2	$-y$ Wheel torque
$-z$ Torque	RCS-2, RCS-4	$+z$ Wheel torque
$+z$ Torque	RCS-1, RCS-3	$-z$ Wheel torque
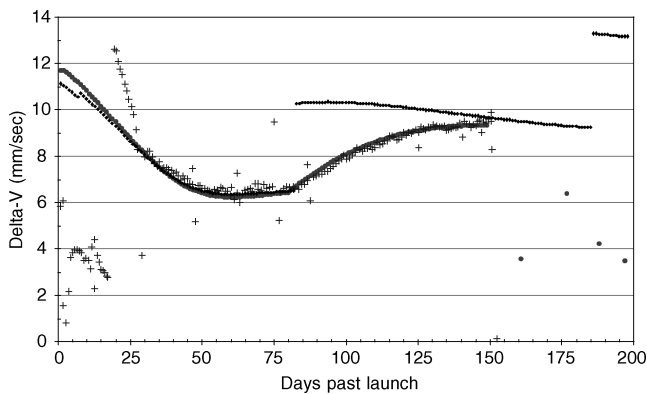
Fig. 3   Daily AMD ΔV total magnitudes: ■, in-flight prediction; +, actuals; and ●, prelaunch.

radiation pressure. When the wheel momentum threshold is reached, generally $2 \text{ N} \cdot \text{m} \cdot \text{s}$, this excess momentum must be unloaded. This AMD event is accomplished by firing the small attitude control thrusters to counteract and unload the angular momentum. Because the thrusters are not balanced, the thrusting imparts a net translational ΔV to the S/C. These events are also referred to as small forces. The thruster suite used to desaturate the wheels consists of four 1-N (0.2-lbf) RCS thrusters, located at the corners of the S/C. These thrusters must provide torque authority in all body axes, and so they are not axially mounted. The thrust-vector direction for each thruster is given in Table 1, in S/C coordinates. The thrusters fire in pairs to desaturate each S/C axis sequentially, but, as mentioned, are not balanced. Note in Table 1 that, because each thruster has a vector component in the $-z$ direction, any RCS thruster firing will result in a net ΔV along the spacecraft z axis.

The y- and z-axis desaturations were most efficient due to the large moment arm. Desaturations of the x axis were relatively inefficient because the moment arm was much smaller, and, therefore, the torque authority was reduced. Because the S/C's x axis was continuously pointed toward Earth during cruise to maintain telecommunications over the high-gain antenna (HGA), desaturations of each axis produced unobservable ΔV components orthogonal to the Earth–S/C direction. Table 2 lists the thruster pairs required to dump momentum from a particular reaction wheel. Although the total translational ΔV, from each desaturation event was small (Fig. 3), the cumulative trajectory perturbation was quite large, on the order of 10,000 km. Therefore, careful trending and calibration were required to meet the delivery accuracy requirements. This also meant that a predicted ΔV profile of all future AMD events had to be included in the trajectory propagation. All RCS thruster pulses during each AMD were recorded in the telemetry stream and downlinked at the beginning or ending of a tracking pass. These data were used in the propagation and determination of the orbit.

The TCMs were performed by using the four 22-N (5-lbf) monopropellant TCM thrusters, which are axially mounted along the

z axis such that they produce ΔV in the $+z$-axis direction. All TCMs were performed in a turn-and-burn mode, which enabled sufficient margin for telecommunications over the medium-gain antenna (MGA). Turns to and from burn attitude are performed by using the reaction wheels. Yaw and pitch control during the burns was enabled by off-pulsing the thrusters, whereas roll control was handled by the RCS thrusters. The MOI burn was performed by using the bipropellant main 695-N engine. At launch, the S/C's total mass was 730 kg including 225 kg of fuel. The expected TCM execution errors are characterized as having a proportional 2% magnitude error with a fixed component of 20 cm/s for ΔV less than 5 m/s. The maneuvers also have a 10% proportional pointing error for ΔV less than 5 m/s, whereas ΔV greater than 5 m/s and less than 20 m/s scale linearly down to 2% for 20 m/s and greater.

Spacecraft Activities

After injection, the S/C was configured to remain in an initial-acquisition, safe-mode attitude. At this attitude, the S/C's low-gain antenna was used to receive uplink signals while the MGA was used for transmission. Following subsystem checkout, the S/C was configured on 9 April 2001 for cruise by altering the attitude and solar array orientation. Almost immediately, the HGA outer gimbal was found to be growing hotter than expected, and so the S/C was returned 8 h later to the safe-mode configuration. The S/C remained in this configuration until it was believed that the solar distance grew far enough to reduce the heating; then the S/C was again reoriented for cruise on 18 April. The gimbal temperatures were again found to exceed the designed values, and so once more the S/C returned to the safe-mode attitude after an 8-h checkout. Finally, on 25 April when the sun–Earth-S/C angle had changed sufficiently, the S/C was configured (as shown in Fig. 2) for cruise with the solar array normal offset 55 deg from the sun. An active thruster calibration took place on 4 May 2001 to characterize the RCS thruster firings used in the AMD events. Following the thruster calibration, the solar array was fixed relative to the S/C body such that the solar array normal sun-offset angle followed the sun–S/C–Earth (SPE) angle within a few degrees. On 10 August, a solar radiation pressure calibration was performed to calibrate more accurately the reflectivity (specular and diffuse) properties of the solar array. On 4 September 2001, the S/C's attitude and solar array were positioned into a low-torque configuration. The S/C held this attitude until two days before encounter, when the solar array was stowed for MOI, meaning that the solar array was stowed against the body within the clasps. After each attitude change, the predicted AMD profile had to be recomputed because each new attitude changed the rate of momentum accumulation and, therefore, the frequency and ΔV characteristics of the autonomous AMD events. Not only did these ΔV affect Odyssey's trajectory, the changes in the solar radiation pressure due to these attitude/solar array changes also affected the trajectory. These changes resulted in significant differences in the expected arrival conditions at Mars.

Tracking Data Types

Navigation and telemetry data were obtained through the near continuous use of the DSN antennas. Because of the trajectory's highly negative declination (from −52 to −42 deg) for the first two months after injection, the S/C was only in view at the Canberra, Australia, DSN complex. Eventually, the Goldstone, California, and finally the Madrid, Spain, complexes were able to track the S/C (declinations from −42 to −23 deg), but tracking was constrained to relatively low elevations for the remainder of cruise (< 30 deg). In general, one DSN contact per day was established, with additional tracking scheduled around critical events. Continuous contact was maintained for the final 50 days of cruise.

The navigation tracking data used for OD included the two-way coherent X-band Doppler (7.2 GHz up/8.4 GHz down), range, and ΔDOR data. The two-way Doppler data measure line-of-sight velocity of the S/C relative to Earth via the Doppler frequency shift in the radio signal. For cruise, the Doppler data were collected by using a 60-s count time. These data typically exhibited noise on the order of 0.02–0.2 mm/s and, consequently, were generally weighted at the 0.1-mm/s level except for the noisier passes of data. The range data

directly measure the relative Earth–S/C distance. The ranging signal was configured to give adequate range signal strength from launch through MOI. The data noise was on the order of 1 m. These data were generally weighted at 3 m. Noncorrelated stochastic range biases per tracking pass were also applied at 5 m to account for station-to-station differences.

In general, the Earth's troposphere and ionosphere delay the X-band signal, and so the radio-metric data must be calibrated to remove their effect. Daily ionospheric and tropospheric calibrations are provided by the Tracking Systems Analysis and Calibrations Group at JPL, who measure the path-length delay through a network of global positioning system (GPS) satellites and GPS receivers. Solar plasma can also affect the X-band signal, but because the view of Odyssey from the DSN is away from the sun, no model was used. Because the media have a pronounced effect on the data at low elevations, the tracking station elevation cutoff was set at 10 deg. The range data are also affected by signal path-length delays at the tracking stations ground electronic systems and the various paths through either of Odyssey's two small deep space transponders (SDST), depending on which S/C antennas are used for uplink and downlink. The SDST delays were calibrated before launch. The station delays are generally measured before and after a ranging pass.

ΔDOR Tracking

The ΔDOR data are formed by the simultaneous observation of Odyssey from two DSN tracking stations separated by an intercontinental baseline. In a ΔDOR observation, the spacecraft signal is received at each of the two stations and the difference in arrival time is measured. This measurement is affected by station clocks, receiver electronics, transmission media, system noise, and other geometric factors. To calibrate systematic effects, an observation of the difference in signal arrival time, or delay, is also made for an angularly nearby quasar. The ΔDOR observable is then formed as the delta between the S/C and quasar signal delays. Instrumentation has been designed and receiver parameters are chosen so that systematic effects for the spacecraft and quasar measurements will nearly cancel. The resulting ΔDOR observable has an expected accuracy of 0.12 ns, one sigma. The leading error sources are system noise, noncanceling instrumental phase shifts, and media fluctuations. A geometric delay accuracy of 0.12 ns corresponds to an angular position accuracy of 4.5 nrad for two stations separated by 8000 km (Ref. 4). This corresponds to S/C position accuracies in the Earth plane-of-sky of approximately 90–680 m for Earth–S/C cruise distances of $20–152 \times 10^6$ km. This measurement error is random for observations taken a day or more apart.

Shortly after Odyssey was observable at the Goldstone complex in June 2001, the ΔDOR observation campaign began using the Goldstone–Canberra baseline. This baseline is also known as the north–south (N–S) baseline because of its ability to ascertain accurate angular measurements in Earth's N–S direction, that is, declination. A single ΔDOR measurement consisted of three 15-min observations (S/C, quasar, S/C). Because of the S/C–Earth geometry, with declination below –25 deg, the Goldstone–Madrid or east–west (E–W) baseline was unavailable because at least a few minutes of station-to-station overlap time are needed to observe the S/C. Beginning on 30 September, this E–W baseline measurement was determined to be viable, but the observation times had to be reduced to 10 min, and the viewing was constrained to very low elevations. These observations consisted of first observing one quasar, then the S/C, and finally a quasar different from the first. The noisy data due to the low elevation that resulted had to be deweighted such that no real benefit was gained by including it in the OD solutions. The ΔDOR campaign consisted of acquiring data at a rate of two points per week until the last three weeks before encounter where the rate went to four per week for a total of 47 measurements (40 N–S and 7 E–W). Only one measurement was lost due to a station transmitter failure unrelated to the ΔDOR measurement.

OD

The JPL Orbit Determination Program's (ODP) pseudo-epoch state least-squares filter was used for determining Odyssey's trajectory and predicting the Mars encounter conditions by estimating the S/C's epoch state and various parameters that model the dynamic environment that influences the S/C's motion. These dynamic influences include the thrusting events of TCMs or AMDs, solar radiation pressure, possible out-gassing events, and the Mars ephemeris within the last several hours before encounter. Stochastic range biases and S/C accelerations were also included in the estimation filter. Once determined using the available tracking data, the trajectory was propagated with a schedule of future AMD ΔV events modeled as impulsive ΔV maneuvers. The contributions of the following errors were considered in the OD covariance: ionosphere, troposphere, station locations, Earth and Mars ephemerides and gravity, polar motion, universal time 1 (UT1), quasar locations, solar pressure areas, and future AMD ΔV.

Thruster Calibrations

Two in-flight thruster calibration activities (one active, one passive) were scheduled to ensure adequate modeling of the thruster perturbation on the trajectory. The calibration was envisioned first as a risk-reduction measure to ensure that no gross computation errors were introduced to the thruster modeling. The second benefit was an increase in the accuracy to which the thrust vector magnitude and direction could be calculated.

The active calibration occurred on 4 May 2001, about one month after launch. This first effort involved slewing the S/C to view the thrusting from several different angles, and there were several operating constraints that affected the design of the calibration. The MGA was limited to 45-deg off Earth-point to maintain telecommunications, and thermal considerations also limited the choice of acceptable attitudes. To minimize changes in configuration, the solar array was constrained to stay in a fixed position for the duration of the event, which also limited the choice of acceptable attitudes from a power perspective. A reaction wheel momentum limit of $3 \text{ N} \cdot \text{m} \cdot \text{s}$ was imposed to prevent the wheels from spinning up to an unsafe rate.

Through iteration, an acceptable design was developed that satisfied all of the constraints and met the objectives of the test. Three nearly orthogonal off-Earth attitudes were chosen to provide observability into the three components of the thrust vector. At each attitude, the thrusters were fired in pairs to spin up, then spin down, sequentially, each reaction wheel. The test totaled 9 h in duration to perform the profile at Earth-point and the three off-Earth attitudes. The goal of this active calibration effort was to characterize completely the magnitude and direction of the thrust vector for each RCS thruster pair. The translational velocity change was measured with the Doppler, and the body and wheel rates were captured in telemetry. The results of the calibration indicated that the predicted models were consistent with the actual thruster performance to within 5%. These results were confirmed with the Doppler analysis, as well as the dynamics analysis.

The passive calibration was performed three months before encounter. The calibration involved all of the data collection, analysis, and interaction between the teams that was required for the active calibration, but was performed only at the Earthpoint attitude. The goal of this test was to confirm that the character of the thrusting had not changed significantly over the course of the mission. Again the results indicated that the models were consistent with the observed performance to within 5%.

Low-Torque Attitude

Once the modeling was shown to be consistent with the performance, an updated momentum management strategy was developed. Because power margin was shown to be sufficient, the first step was to fix the solar array orientation to minimize the disturbance torque. Instead of a fixed sun-offset angle of 45 deg as planned before launch (baseline attitude), the solar array was fixed with respect to the S/C body to follow the SPE angle, thereby reducing the solar torque. To further reduce the effects of the AMD events on orbit determination during the final two months of interplanetary cruise, the navigation team requested the attitude and solar array position be adjusted to place the center of pressure as close to the S/C's center of mass as

possible. This low-torque attitude nearly eliminated the buildup of momentum and, thus, minimized the number of AMD events during the most critical portion of cruise. The adoption of the low-torque attitude late in cruise reduced the desaturation frequency from twice per day to twice per month. This configuration worked so well that no autonomous desaturations occurred during this time. Only forced desaturations occurred before the four following activities: MOI checkout (6 September), TCM-3 (17 September), TCM-4 (12 October), and the S/C reconfiguration into the MOI attitude (22 October). In addition to the minimizing of the desaturation frequency, the ΔV per event was minimized (Figs. 3 and 4). Also shown in Fig. 4 is the desaturation frequency that was predicted prelaunch. The prelaunch model was reasonably accurate, but the operations in-flight changed significantly from the plan.

Covariance Analysis

Prelaunch, a covariance analysis was performed to determine Odyssey's navigation targeting capability at TCM-4. This analysis included the expected accumulation of Doppler, range, and ΔDOR data and similar filter assumptions discussed earlier. Table 3 lists the expected flyby altitude errors for the prelaunch analysis. The errors have been broken down into the OD only (all error models except AMDs), AMD ΔV prediction errors, and expected TCM-4 execution errors. The AMD predicted error model accounted for random velocity errors with a once per day frequency. In operations, the AMD ΔV estimates were showing consistent biases of 5–10%, and so the covariance analysis was updated to include this bias error (with 10% uncertainty). Treated in this way, the AMD ΔV errors became the dominant error source. Table 3 shows a comparison of the in-flight error model assumptions (original baseline attitude case) on the target altitude covariance. Also note that, aside from slight filter assumption changes, the TCM-4 was moved back two days from the prelaunch plan. With these new assumptions, the altitude uncertainty of the baseline attitude case increased by 24% over the prelaunch case. Because the low-torque attitude profile dramatically reduced the quantity of predicted AMD ΔV, the low-torque case in Table 3, the attitude error improved by 14% over the prelaunch case and by 31% over the baseline attitude case. For comparison, a no-ΔDOR baseline attitude case is also listed in Table 3.
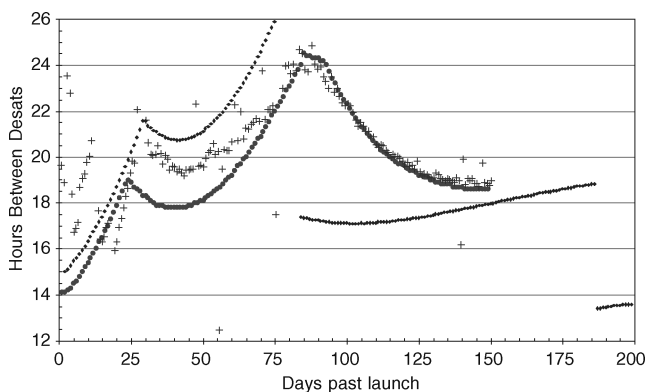

Fig. 4 Frequency of AMD events during cruise; after S/C low-torque attitude was configured (approximately 150 days after launch), no autonomous desaturations occurred: ■, in-flight prediction; +, actuals; and ●, prelaunch.

Filter Strategy

In addition to a baseline filter case, OD solution consistency was routinely evaluated through a battery of filter strategies and data combinations. The approach to the OD problem with regard to the challenges presented beforehand was to define a set of filtering configurations that would encompass the realm of possible modeling uncertainties. This approach also included unrealistic strategies. The goal of this approach was to understand how these filtering strategies influenced the solutions by determining the sources of solution differences. The unrealistic strategies were used to cover extreme possibilities that may reveal modeling problems that could have been masked by the nominal filtering strategies.

Software tools were built to visualize and trend the results of these many cases and to help decipher the causes of solution discrepancies. Finally, OD strategies and results also were regularly reviewed (up to daily) in the two months before MOI by the Navigation Advisory Group (NAG) at JPL.

Throughout cruise, we observed that the beginning and end of the fit two-way Doppler data would exhibit slopes. Much effort went into finding the cause of these patterns. The S/C dynamic models and media calibrations were reevaluated. Solar pressure and the small-force AMD events were found to be noncontributing factors. Media parameters were estimated, but found to be unrealistically large. A white-noise three-axis stochastic gas-leak acceleration model was routinely estimated to account for possible unmodeled accelerations acting on the S/C. Several batch lengths of from 2 h to 2 days were used with an a priori uncertainty on the order of 10–20% of the solar radiation pressure value (≈ 60–80 nm/s^2). The only significant gas-leak acceleration estimates were in the Earthline component.

During the TCM-2 data arc, a couple passes of Doppler residuals such as those shown in Fig. 5 exhibited a peculiar sawtooth pattern. Because it appeared that we were having problems fitting the data without the gas-leak acceleration estimation, we became concerned that this may have been more evidence of serious problems in the S/C modeling, the SDST, DSN hardware, or the ODP. Several DSN and NAG experts helped analyze these unusual patterns, but no definitive explanation was found. The DSN tracking procedures for Odyssey had been to follow the S/C's downlink frequency within a fairly tight bandwidth by periodically ramping the uplink signal. It was believed that this ramping of the signal could have contributed to this problem, especially if the values of the ramp rates were being truncated, but no evidence of this was found. In the case that these data were incorrect, our procedures were to remove the data. However, it was determined that the data had little effect on the OD solutions, especially due to the signatures' high-frequency nature.

Several passes of Doppler residuals and fewer passes of range residuals were exhibiting more anomalous signatures. The low-elevation data, especially at the Madrid complex, were suspected to be strongly influenced by media. Unlike the high frequency of the sawtooth pattern, these longer period fluctuations in the Doppler data were found to shift Odyssey's OD solutions by orders of 1σ in the B plane from one hour to the next. Tropospheric and ionospheric calibrations for Odyssey were generally computed and delivered twice per week, and these products included predicted calibrations to cover the times between deliveries. During the time of the TCM-3 design (early September), inconsistencies on the order of 2σ in the $B \cdot R$ direction were found between OD solutions that included ΔDOR to those that did not. When a new troposphere calibration delivery (received just after the OD027 delivery for TCM-3 design) was used in the OD, these inconsistencies were removed. Furthermore, when

Table 3 TCM-4 encounter altitude delivery errors

At TCM-4 data cutoff (MOI-16 days), 1σ	Prelaunch, km	Baseline attitude no ΔDOR, km	Baseline attitude ΔDOR, km	Low torque, km
OD only	6.4	7.0	3.6	5.6
AMD predicts only	1.0	8.2	8.2	0.3
OD Plus AMD predictions	6.5	10.8	9.0	5.6
TCM execution errors only	4.4	3.6	3.6	3.6
Total delivery accuracy, 1σ	7.8	11.4	9.7	6.7
Total delivery accuracy, 3σ	23.5	34.1	29.1	20.0

Sawtooth: C = 0   G = F   N = 4493   M = 0.000610607   R = 0.0041087   S = 0.00406307
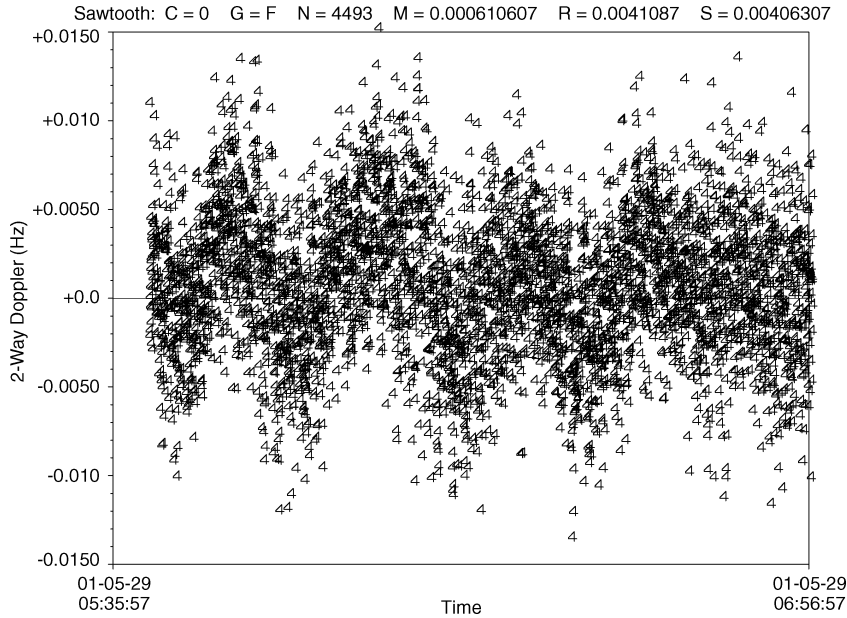
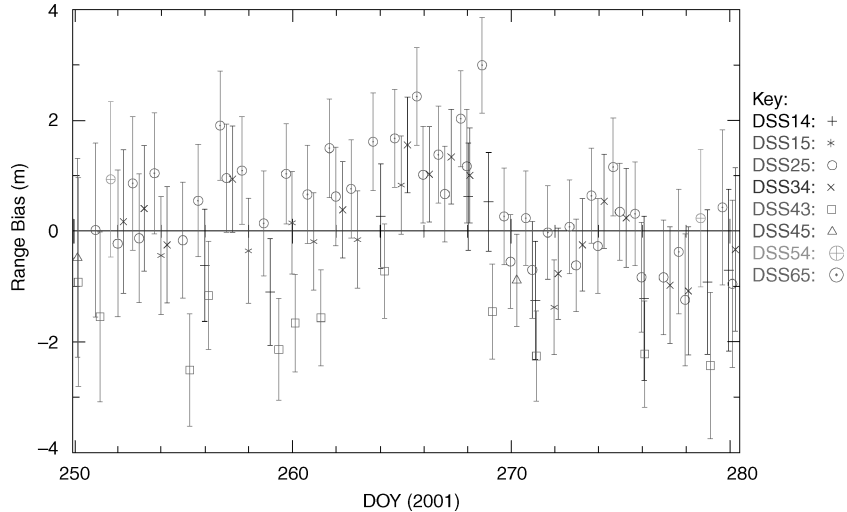Fig. 5   Sawtooth signature in 1-s two-way Doppler residuals from Canberra DSN station.

Fig. 6   Estimated range biases per tracking pass.

these calibrations were included in the ΔDOR solutions, such as OD027, the shift was smaller, approximately 1σ. In general, solutions that did not include ΔDOR data would exhibit larger changes when new media calibrations were delivered. Including ΔDOR data stabilized the solutions. Because there was a lack of media observations using the GPS survey in the line-of-sight direction to Odyssey from Madrid, the calibrations were found to not model the troposphere and ionosphere correctly for the Madrid passes. To verify the media's affect on the radio signal, a few DRVID measurements were taken using the S/C's DOR tones to measure the media's total electron content (TEC). Because the ranging measurement's code modulated on the carrier signal experiences a positive group delay and the carrier phase experiences a negative phase delay, DRVID is a direct measurement of the TEC along the signal path.[5] The DRVID measurements verified that the disturbances to the radiometric data at Madrid were caused by media (ionosphere and/or solar plasma). It was also known that solar activity during this time was high and that there were reports of several coronal mass ejections.

Figure 6 shows range biases of ± 3 m estimated during a TCM-4 data arc. Madrid's Deep Space Station (DSS) 65 was found to have biases of 1–2 m, whereas Canberra's DSS-43 exhibited biases of from −1 to −2 m. The other DSS antennas generally showed biases of 1 m or less. Generally, all pass biases were resolved down to ± 1 m. These station relative bias variations were typically seen in the OD solutions because Madrid and Goldstone came into view of Odyssey.

The ΔDOR residuals for the N–S baseline generally fit down to the 0.12 ns applied weight. The E–W baseline, on the other hand, could not fit down to this level. These data generally fit to an accuracy of 1 ns. The E–W data were determined to be highly influenced by inadequate media coverage at the low elevations south of Madrid and, thus, were not included in the OD solutions. Figure 7 shows a comparison of ΔDOR solution (including Doppler and range) residuals to a Doppler and range-only solution (no ΔDOR). The ΔDOR residuals in Fig. 7 have been mapped to Earth plane-of-sky distances in the second to last month before MOI. At the S/C–Earth distances during this time, ΔDOR fixes the S/C's position to under 500 m relative to the Earth's N–S direction. For comparison, the ΔDOR data were passed through the Doppler and range-only solution. Here the S/C's trajectory shows N–S position residuals of 1–5 km from the ΔDOR measurements. The semimajor and semiminor axes of the S/C's state covariance mapped to the Earth's plane-of-sky is also shown for comparison. Aside from the first two points, the ΔDOR pass-through residuals of the Doppler and range solution show consistency with the plane-of-sky covariance.

In the month before the design of TCM-3, several filter approach strategies were identified for routine inspection during the days leading up to MOI. A set of 13-cases was developed to encompass realistically the realm of possible OD solutions by covering areas of concern. These concerns included mismodeling of nongravitational accelerations or forces on the S/C, data-type inconsistencies, and
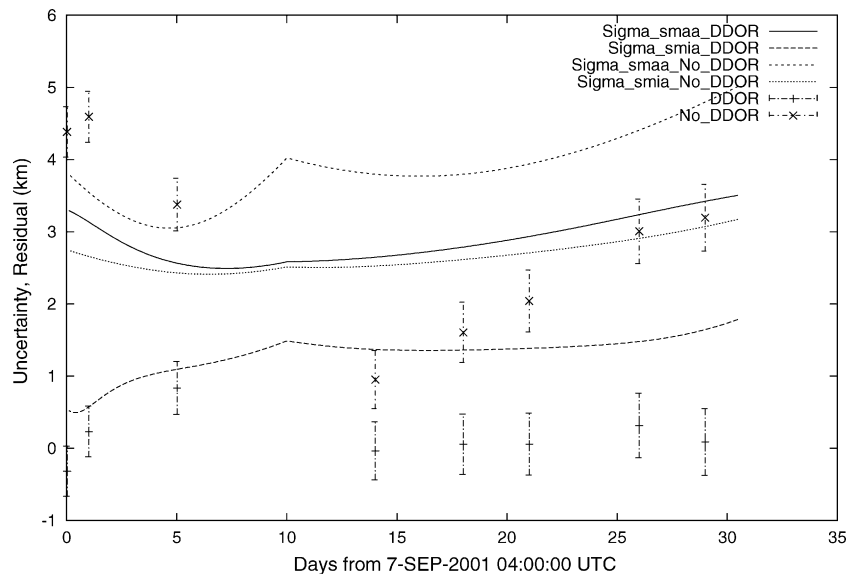
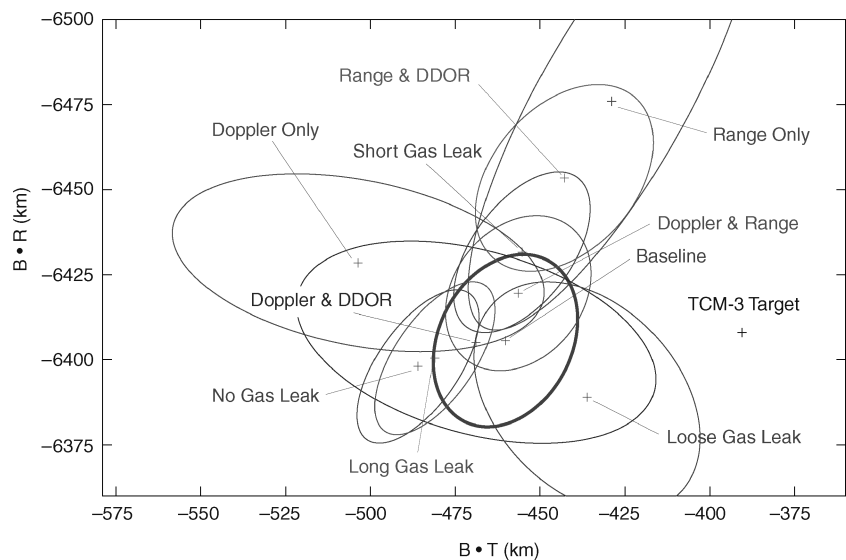Fig. 7 ΔDOR residuals with respect to mapped Earth plane-of-sky convariance.

Fig. 8 Comparison of filter strategies during post-TCM-3 analysis (1σ).

data problems. The baseline filter strategy included the Doppler, range, and ΔDOR data, respectively, with the nominal weights of 0.1 mm/s, 5 m, and 0.12 ns and an elevation cutoff of 10 deg (later updated for TCM-4 design to 15 deg). The filter setup included estimating one scaling factor on the ΔV per axis desaturation, the white-noise stochastic gas-leak acceleration with a batch length of 12 h and process noise of 5 nm/s^2 in the Earthline component and 1 nm/s^2 in the orthogonal directions, 50–100% uncertainties applied to the specular and diffuse reflective properties of the solar array and bus in the solar radiation pressure model, and white noise stochastic pass-dependent range biases with process noise of 5 m. The following cases departed from the baseline only in the change of the concerned model or data. The cases included loosening the a priori uncertainties on the desaturations, on the solar radiation pressure parameters, or stochastic gas leaks and changing the batch length (longer or shorter) or removing the gas leak from the filter. The Appendix (Table A1) gives the nominal a priori uncertainties for the estimated and considered parameters in the baseline case. Tight and loose a priori uncertainties are also listed in the Appendix for the alternative cases. Data-type variations included the following cases: Doppler only, Doppler and range, and Doppler and ΔDOR. The cases that addressed data problems included deweighting the Doppler data by two times, changing the elevation cutoff to 15 deg, and removing entire passes of Doppler data that exhibited unusual signatures.

With the continuous tracking data available during the last two months before MOI, trending of the 13 cases with short, medium, and long data arc lengths of 1–4, 4–9, and 9–12 weeks, respectively, were performed on a near daily basis. Several other nonstandard strategies were performed 2–3 times per week. The strategies included the following cases: applying loose range bias a priori, range only, range and ΔDOR, estimating Doppler biases, and an enhanced filter setup. The enhanced filter incorporates the estimation of Earth's polar motion and rotation and data errors from sources such as the ionosphere, troposphere, and station or S/C transponder biases into the filter as stochastic processes.[6]

Figure 8 shows an example of how the various filter strategies compare in the MME B plane at the time of the post-TCM-3 solutions. Compared to the baseline strategy, the Doppler-only solutions were found to reside approximately 1σ or more to the left (in the $B \cdot T$ direction), Doppler-and-range solutions were 1σ above (in the $B \cdot R$ direction), range-only solutions were more than 1σ above, no-gas and long gas-leak solutions drifted down to the left, and the short gas-leak drifted up to the right approximately 1σ. The addition of the ΔDOR to the Doppler or range-only cases brought the solution closer to the baseline. The enhanced filter solution (not shown) was within 1σ of the baseline; however, several parameter estimates, especially media corrections, were unrealistically large. A comparison of the expected B-plane error ellipses at the time of the TCM-4
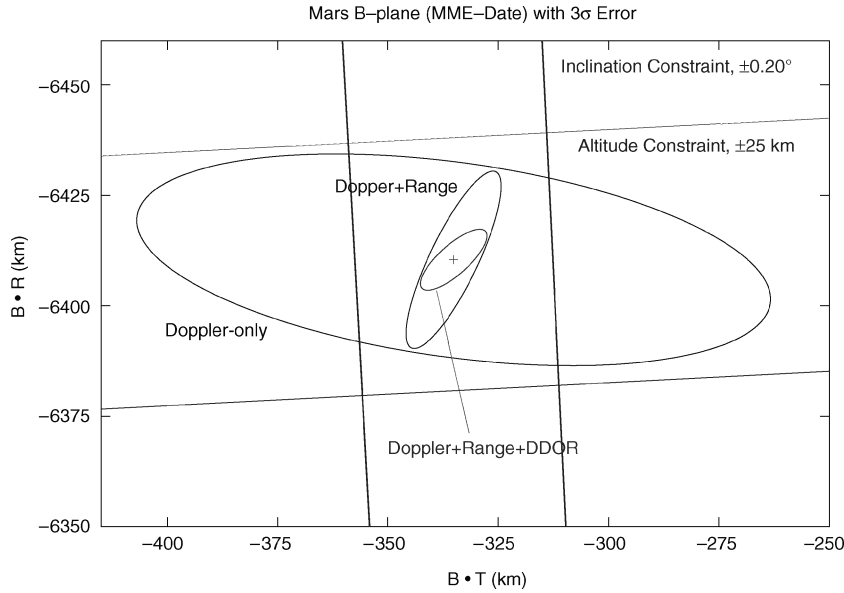
Fig. 9 Comparison of trajectory knowledge (3-σ) at time of TCM-4 design (MOI-16 days) with different data-type combinations.
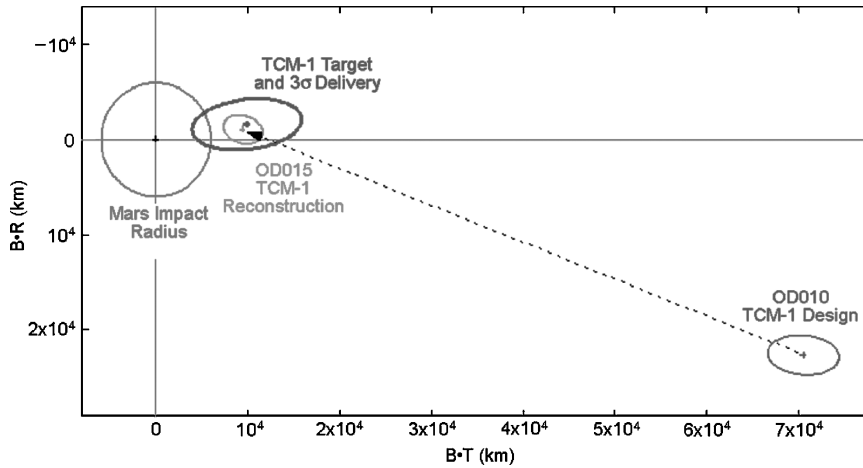

Fig. 10 TCM-1 target and 3σ delivery dispersion and achieved results.

solution (MOI-16 days) for different data combinations is shown in Fig. 9. Figure 9 demonstrates the strength of the ΔDOR data to determine Odyssey's trajectory when combined with the Doppler and range data types, especially in the altitude direction ($\boldsymbol{B} \cdot \boldsymbol{R}$).

Results

After accumulating several minutes of Doppler data following separation from the launch vehicle's third stage, the Multi-Mission Navigation Team at JPL determined Odyssey's flight path and transferred the estimated state vector to the Odyssey Navigation Team. With several more hours of Doppler and range measurements, it was determined that the Delta 2 launch vehicle had injected the S/C onto a trajectory that would take it nearly 2σ away from the designed target.[1] This off-nominal performance fortuitously put Odyssey on a favorable trajectory. Instead of the expected ΔV of 15.4 m/s to remove the bias and bring Odyssey closer toward Mars, TCM-1 only required approximately 3.6 m/s. Not only did it result in a substantial propellant savings, the first flight-path correction, TCM-1, was delayed to 46 days (23 May) after launch instead of the planned launch + 8 days.

TCM-1 Design

To support the TCM-1 maneuver design, the OD team collected tracking data up to 13 days before the maneuver execution. Several S/C events perturbed the trajectory in the time leading up to the TCM-1 design. In addition to the 46 AMD events, these in-

cluded the active RCS thruster calibration, the THEMIS Earth–Moon calibration, and a safing event, which lost a few packets of AMD data and produced a higher frequency of desaturations. In addition to an acceleration presumably caused by the escaping of trapped gas or surface material out-gassing experienced shortly after launch, a clear indication of out-gassing appeared during the turn for the THEMIS calibration. The equivalent ΔV amounted to approximately 1.5 mm/s. The epoch of the data arc was advanced past the final S/C transition to cruise orientation on 25 April. A TCM-1 of 3.6 m/s was designed to move the S/C 65,000 km closer to Mars and change arrival time by 3.5 h earlier. Because TCM-1 and the next burn, TCM-2, were designed and optimized together, TCM-1 did not target the final encounter aimpoint. Based on radiometric data and burn telemetry, the maneuver was determined to have accurately achieved the desired ΔV magnitude, but the pointing was off approximately 3 deg, about a 1σ error. (See Table 4 for maneuver statistics.) Following the TCM-1 burn, the predicted attitude and, thus, the predicted AMD events were changed to reflect new assumptions. This resulted in a B-plane shift of approximately 1000 km closer to the desired TCM-1 aimpoint. Table 5 shows a comparison of the TCM-1 B-plane target against that achieved through the TCM-1 reconstruction. Figure 10 shows the movement of the S/C's trajectory resulting from the TCM-1 burn mapped to the time of encounter in the MME B plane. In Fig. 10, the TCM-1 target and expected 3σ maneuver uncertainties are compared to that achieved.

Table 4   Maneuver reconstructions

Date executed, UTC-SCET[a]	Design (EME-2000)[b]	Reconstruction	Sigma	Deviation from design
		TCM-1		
23 May 2001 17:30				
ΔV, m/s	3.5578	3.5628	0.014 (0.40%)	0.14%
α, deg	−28.9760	−29.3478	0.209	−0.372
δ, deg	−0.5539	−3.3952	0.204	−2.841
Total pointing error				2.87 deg
		TCM-2		
2 July 2001 16:30				
ΔV, m/s	0.8992	0.9093	0.073 (0.25%)	1.12%
α, deg	−21.171	−22.094	0.121	−0.927
δ, deg	8.343	8.619	0.171	0.276
Total pointing error				0.95 deg
		TCM-3		
17 Sept. 2001 04:00				
ΔV, m/s	0.4496	0.4630	0.002 (0.37%)	2.98%
α, deg	87.9686	84.1285	0.548	−3.840
δ, deg	−63.5344	−63.3219	0.079	0.213
Total pointing error				1.73 deg
		TCM-4		
12 Oct. 2001 04:00				
ΔV, m/s	0.0772	0.0772	0.001 (1.2%)	−0.04%
α, deg	−174.5770	−174.5536	0.197	−0.023
δ, deg	10.8916	10.8298	0.199	−0.062
Total pointing error				0.066 deg

[a]UTC-SCET, coordinated universal time–spacecraft event time.   [b]EME-2000, Earth mean equator of 2000.

Table 5   Mars B-plane aim point and (1σ) delivery results Mars centered, Mars mean equator (MME) date: 24 Oct. 2001 ET

Solution	$B \cdot R$, km	$B \cdot T$, km	TOF, ET-SCET[a]
		Injection	
Target and delivery	45,572 ± 75,000	439,690 ± 190,000	25 Oct. 2001 23:43:40
Postinjection / TCM-1 design (OD010)	22,646 ± 693	70,496 ± 1291	06:28:09 ± 404 s
		TCM-1	
Target and delivery	−1565 ± 904	9972 ± 1977	02:56:58 ± 730 s
Post-TCM-1	−693 ± 652	8178 ± 1061	02:46:10 ± 356 s
Difference	871 (+0.96σ)	−1794 (−0.91σ)	−648 s (−0.89σ)
TCM-2 design (OD015)	−1064 ± 1496	9459 ± 2140	02:49:15 ± 696 s
		TCM-2	
Target and delivery	−6825 ± 518	46 ± 998	02:30:00.3 ± 214 s
Post-TCM-2	−6913 ± 363	−98.0 ± 480	02:29:51.7 ± 145 s
Difference	−88 (−0.17σ)	−144 (−0.14σ)	−8.6 s (−0.04σ)
TCM-3 design (OD027)	−7619 ± 19	221 ± 23	02:30:41 ± 7 s
		TCM-3	
Target and delivery	−6408 ± 38	−391 ± 53	02:30:00 ± 14 s
Post-TCM-3/TCM-4 design (OD034)	−6430.2 ± 4.2	−463.9 ± 5.6	02:30:08.1 ± 1.3 s
Difference	−22.2 (0.58σ)	−72.9 (1.4σ)	8.1 s (0.58σ)
		TCM-4	
Target and delivery	−6407.00 ± 5.3	−391.00 ± 8.3	02:29:57.7 ± 1.7 s
Achieved	−6408.00 ± 0.04	−395.39 ± 0.06	02:29:58.3 ± 0.004
Difference	−1.00 (−0.19σ)	−4.39 (−0.5σ)	0.6 s (0.4σ)

[a]ET-SCET, ephemeris time–spacecraft event time.

TCM-2 Design

The data cutoff for the TCM-2 design solution (OD015) was 11 days before the execution of TCM-2 on 2 July. The data arc began after the TCM-1 burn and included five N–S ΔDOR measurements, several passes of Goldstone, and three passes of Madrid. When the error contributions from the predicted AMD were considered, ΔV inflated the B-plane statistics by approximately six times, and so these errors were removed in the comparison of the various OD solutions strategies. With these errors removed, it was found that the inclusion of the ΔDOR data into the OD baseline strategy consistently moved the solution approximately 1σ away from the Doppler and range solution.

TCM-2 executed with a ΔV of 0.9 m/s to move the S/C's mapped B-plane encounter conditions closer to the final aimpoint over the north pole of Mars (Fig. 11). Because of the expected maneuver errors, TCM-2 was designed to lessen the probability of impact by biasing the trajectory away from the final aim point by approximately 1000 km. The maneuver listed in Table 4 was reconstructed to be an overburn of approximately 1% in ΔV magnitude and 1-deg error in pointing. TCM-2 achieved its target with 0.2σ of the delivered statistics listed as the post-TCM-2 solution in Table 5.

TCM-3 Design

After the design of TCM-2, two changes for the remaining AMD ΔV profile were adopted. These included the changes to the future ΔV from the fixing of the solar array orientation with respect to the S/C body and changing the S/C configuration into the low-torque attitude after 4 September. These changes, especially the low-torque,
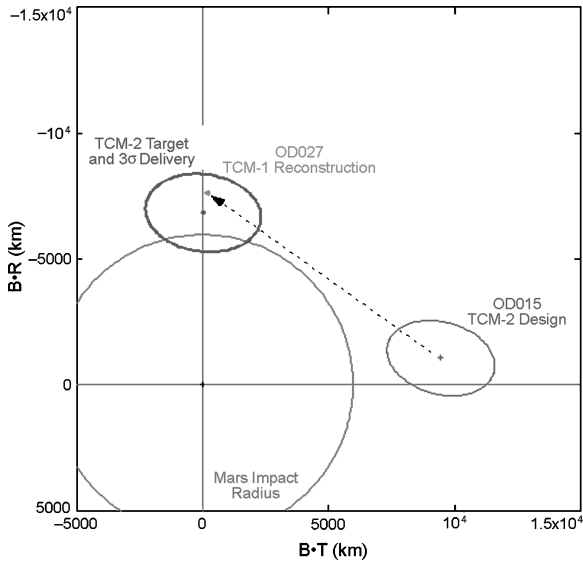
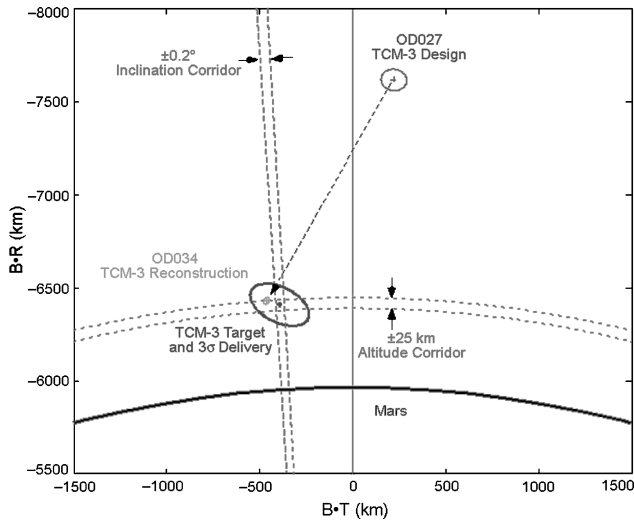**Fig. 11 TCM-2 target and 3σ delivery dispersion and achieved results.**

Fig. 12 TCM-3 target and 3σ delivery dispersion and achieved results.

caused the trajectory mapping to move deterministically upward away from the TCM-2 target about 840 km. The analysis of the active thruster calibration had computed small RCS thruster misalignments and differences in thrust levels from the nominal values. This analysis was used to adjust the AMD ΔV values with respect to the raw telemetry. Further analysis through the OD process showed that these adjustments were closer to those observed, so this small-force formulation, referred to as 3aeR2, was used in the solutions. Later, after the passive thruster calibration took place, the thruster vectors were again adjusted in version 3aeR2-ptcal.

The OD solution (OD027) for the design of TCM-3 used data up to seven days before the burn executed. TCM-3 executed on 17 September with a ΔV of 0.5 m/s to move the S/C's trajectory to the final aimpoint for MOI as shown in Fig. 12. The desired inclination and altitude corridors are shown in Fig. 12. The direction of the ΔV was nearly orthogonal to the Earthline direction, which made it challenging for the OD team to determine the performance quickly. After a few days of tracking, the burn was determined to be 3% over in magnitude and nearly 2-deg off in pointing. The error in the pointing may have been caused by the rate damping of the attitude control system after the maneuver. Although TCM-3 achieved the upper boundary requirement on the altitude corridor, it missed the target by approximately 1.5σ, mainly in the $\boldsymbol{B \cdot T}$ or inclination direction.

TCM-4 Design

The tracking data for the design of TCM-4 (OD034) were cut-off five days before the burn's 12 October execution. There were 82 solutions computed to support TCM-4. From the time since the TCM-3 design, 800 solutions had been generated. The epoch of the baseline solution used for TCM-4 design began on 7 September after the transition to the low-torque configuration and the MOI checkout activity on 6 September. Aside from estimating the TCM-3 burn and its associated RCS firings (forced desaturation before, and rate damping afterward), these data arc maximized the amount of tracking data while the S/C was minimally influenced by dynamic events. The various OD solutions showed remarkably good agreement. A small 8-cm/s TCM-4 was designed to achieve the final aimpoint. Figure 13 shows the path of TCM-4 to the final aimpoint in the MME B plane with the expected 3σ delivery statistics fitting well inside the targeted corridor.

TCM-5 Go/No-Go Decision

There were concerns that TCM-4 was too small to be adequately executed on Odyssey because of quantization effects in the propulsion system. However, TCM-4 performed flawlessly with negligible error (Table 4). Following the execution of TCM-4, the Navigation Team presented daily OD updates to the project and NAG. Figure 14 shows the process of determining Odyssey's final delivery at Mars
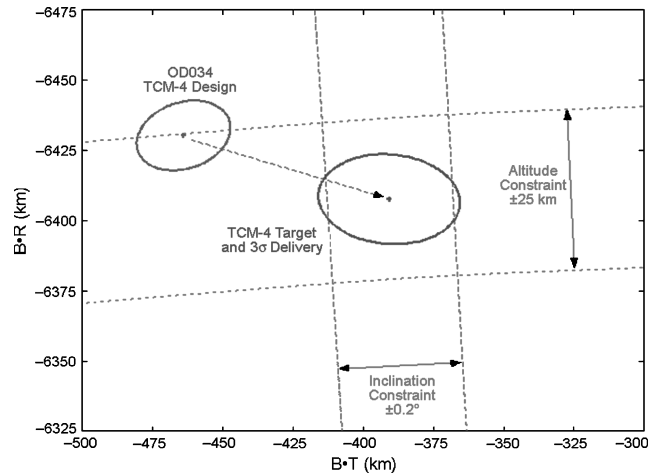

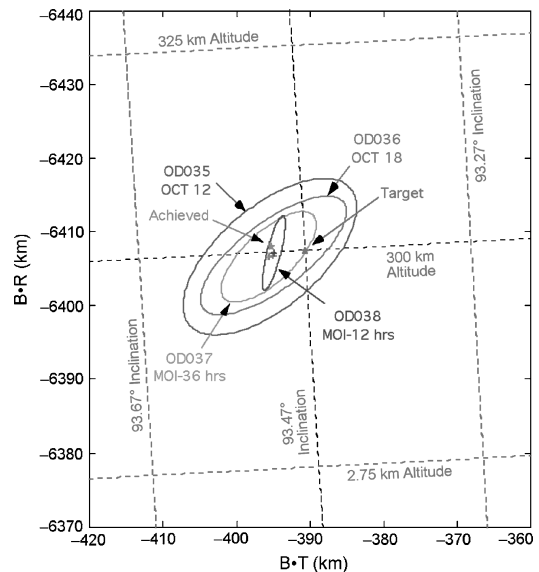**Fig. 13 TCM-4 target and 3σ delivery dispersion.**

Fig. 14 TCM-4 target and 3σ delivery dispersion and achieved results.

by showing the consecutive *B*-plane results following TCM-4 at MOI-12 days (12 October) MOI-6 days (18 October), MOI-36 h, MOI-12 h, and finally at encounter.

The decision of whether to perform a TCM-5 maneuver was based on the *P*2 altitude. The periapsis altitude during MOI was expected to be 328 km, which was well out of the Martian atmosphere. Because of the natural drop in periapsis radius due to the pitchover MOI burn, the target periapsis altitude at *P*2 was 300 km, with an expected altitude uncertainty of 15-km 3σ. To provide ample margin, a reasonably large uncertainty of 50 km was used to define the TCM-5 go/no-go criteria. The region of concern was an altitude below 200 km, which would place the S/C within the sensible Mars atmosphere. Thus, the criteria stated that if the solution plus the 50-km uncertainty dipped below 200 km at *P*2, then a TCM-5 maneuver would be executed to raise the periapsis altitude. Two opportunities for TCM-5 were scheduled at MOI-24 h and MOI-6.5 h. The decisions on whether to perform the burn were made 2.5 and 2 h, respectively, beforehand. These decisions were based on OD updates with the data cut off, respectively, 9.5 (MOI-36 h), and 4.5 (MOI-12 h) hours earlier. Because the estimated periapsis altitude remained within 1 km of the 300-km target (at *P*2) during these times, the 50-km altitude margin never approached the 200-km limit, and as a result, TCM-5 was not executed at either opportunity.

With respect to the TCM-4 delivery statistics, the achieved conditions were approximately 0.2σ (-1 km) high in the $\boldsymbol{B} \cdot \boldsymbol{R}$ and 0.5σ (-4 km) to the left in the $\boldsymbol{B} \cdot \boldsymbol{T}$ directions and 0.4σ (0.6 s) late (Table 5). The achieved altitude at *P*2 was 0.7 km high and the inclination was off 0.04 deg (Table 6).

Conclusions

With the help of the ΔDOR data and the low-torque attitude, the Odyssey Navigation Team was able to overcome the challenges presented to the OD processes. These challenges included the effects of the routine AMD small forces and the tracking data problems on the OD solutions. The ΔDOR measurements complemented the traditional Doppler and range data by improving the S/C's out-of-ecliptic-plane position component, which was necessary for achieving the encounter conditions. The low-torque attitude effectively removed the desaturation ΔV as being a significant error contributor in the OD solutions, especially for the final targeting maneuver, TCM-4. The inspection of the final TCM design solutions through the routine evaluation of the many filter strategies helped our understanding of how the dynamic models and radiometric data quality can affect the OD solutions. These improvements resulted in arrival conditions over the north pole of Mars well within 1σ of the designed values. The achieved altitude above the north pole was less than 1 km away from the 300-km target altitude.

Table 6 Comparison of achieved altitude and inclination conditions to target 1σ

Aim point	Altitude, km	Inclination, deg
Flyby target	404.50 $\pm$ 5	93.4690 $\pm$ 0.07
Achieved	405.23 $\pm$ 0.043	93.5102 $\pm$ 0.0006
Difference	0.73 (0.14σ)	0.041 (0.6σ)
P2 target	300.00 $\pm$ 5	93.4670 $\pm$ 0.07
Achieved	300.73 $\pm$ 0.043	93.5102 $\pm$ 0.0006
Difference	0.73 (0.14σ)	0.043 (0.6σ)

Appendix: Filter Strategies

Table A1 Estimated and considered parameter a priori uncertainties and data weights

Filter parameters	A priori uncertainties	Nominal	Tight	Loose
Estimated parameters				
Position		10^6 km		
Velocity		1.0 km/s		
Solar pressure				
Solar array	Specularity	50%	25%	100%
	Diffusivity	30%	15%	100%
Drag flap	Specularity	50%	25%	100%
	Diffusivity	50%	25%	100%
Bus-*X* face				
Bus-*Y* face	Specularity	100%	50%	200%
Bus-*Z* face				
HGA	Diffusivity	50%	25%	100%
TCMs				
Magnitude		2% + 0.020 m/s		
Direction	0.04 < ΔV < 5 m/s	10%		
	5 < ΔV < 20 m/s	10% − 2% (linear)		
	ΔV > 20 m/s	2%		
AMD ΔV[a]	1 per entire	20%	10%	100%
Impulsive ΔV in S/C coordinate	S/C *x*−*y*−*z* desaturation			
Stochastic parameters				
Three-axis acceleration (gas leak) in S/C coordinate				
Spherical		5e−12 km/s^2	1e−12 km/s^2	1e−11 km/s^2
Correlation time		0		
Batch length		2 hr–2 day		
Range bias		5 m	4 m	1000 m
Correlation time		0		
Batch length		per pass		
AMD ΔV[a], small force file	One scale per S/C axis desaturation	20%	10%	100%
AMD ΔV[a], small force file	Three-axis scale per S/C axis desaturation	20%	10%	100%
Considered parameters				
Predicted AMD ΔV in S/C coordinate				
X	Acceleration	1.1 mm/s = 13e−12 km/s^2		
Y	per day	0.8 mm/s = 9.3e−12 km/s^2		
Z		0.9 mm/s = 10e−12 km/s^2		

(Continued)

Table A1   Estimated and considered parameter a priori uncertainties and data weights (continued)

Filter parameters	A priori uncertainties	Nominal	Tight	Loose
Ionosphere				
Day		3 cm		
Night		1 cm		
Troposphere				
Wet		2 cm		
Dry		1 cm		
Polar motion, X, Y coordinate		5 cm (7.5 nrad)		
UT1		15 cm (0.32 ms)		
Ephemerides				
Earth		JPL DE405 covariance		
Mars		JPL DE405 covariance		
Station locations		JPL DSN Full covariance		
Quasar locations, RA, Dec		5 nrad		
Solar pressure, all areas	Area, m^2	2.50%		
Gravity parameter				
Earth, km^3/s^2		$2.500000E-03$		
Moon, km^3/s^2		$1.476000E-06$		
Mars, km^3/s^2		$2.621440E-03$		
Data weights				
Two-way X band				
Doppler		0.1 mm/s	0.05 mm/s	0.2 mm/s
Range		3 m	1 m	100 m
ΔDOR		0.12 ns	0.12 ns	0.36 ns
Data arc length				
Short		1–4 week		
Medium		4–9 week		
Long		9–12 week		

[a]AMD ΔV, one method used (impulsive ΔV, stochastic ΔV magnitude scale per desaturation, or three-axis stochastic ΔV scaling per desaturation.

References

[1]Mase, R. A., Antreasian, P. G., Bell, J. L, Martin-Mur, T. J., and Smith, J. C., Jr., "Mars Odyssey Navigation Experience," *Journal of Spacecraft and Rockets*, Vol. 42, No. 3, 2005, pp. 386–393.

[2]Smith, J. C., Jr., and Bell, J. L., "2001 Mars Odyssey Aerobraking," *Journal of Spacecraft and Rockets*, Vol. 42, No. 3, 2005, pp. 406–415.

[3]"2001 Odyssey Navigation Plan and Trajectory Characteristics," Final Version, Jet Propulsion Lab., JPL Rept. D-16001, 722-202, California Inst. of Technology, Pasadena, CA, March 2001.

[4]Border, J. S., "Expected Delta-DOR Measurement Performance for the Mars 01 Mission," Jet Propulsion Lab., Interoffice Memorandum 335-00-03-A (JPL Internal Document), California Inst. of Technology, Pasadena, CA, 11 Aug. 2000.

[5]Thornton, C. L., and Border, J. S., "Radiometric Tracking Techniques for Deep-Space Navigation," Monograph 1, *Deep-Space Communications and Navigation Series*, Jet Propulsion Lab., JPL Publ. 00-11, California Inst. of Technology, Pasadena, CA, Oct. 2000.

[6]Estefan, J. A., Pollmeier, V. M., and Thurman, S. W., "Precision X-Band Doppler and Ranging Navigation for Current and Future Mars Exploration Missions," American Astronautical Society, AAS Paper 93-250, Aug. 1993.

R. Mase
Guest Editor